CSIRO PUBLISHING

Reproduction, Fertility and Development, 2017, **29**, 2269–2276
https://doi.org/10.1071/RD16267

Pannexin channels increase propidium iodide permeability in frozen–thawed dog spermatozoa

J. L. Torres[B], *J. Palomino*[A], *R. D. Moreno*[B] *and M. De los Reyes*[A,C]

[A]Laboratory of Animal Reproduction, Faculty of Veterinary Sciences, University of Chile, Casilla 2, Correo 14, La Granja, Santiago, Chile.
[B]Physiology Department, Biological Sciences Faculty, Pontifical Catholic University of Chile, Alameda 340, Santiago, Chile.
[C]Corresponding author. Email: mdlreyes@uchile.cl

Abstract. Pannexins (Panx) are proteins that form functional single membrane channels, but they have not yet been described in dogs. The aim of the present study was to detect Panx1, Panx2 and Panx3 in frozen–thawed dog spermatozoa using flow cytometry and immunofluorescence analyses, evaluating the relationship of these proteins with propidium iodide (PI) in frozen–thawed spermatozoa. Fresh and frozen–thawed dog spermatozoa from eight dogs were preincubated with 3 μM PI with or without 15 μM carbenoxolone (CBX) or 1 mM probenecid (PBD), two Panx channel inhibitors, and then incubated with rabbit anti-Panx1, anti-Panx2 and anti-Panx3 antibodies (1 : 200). Panx immunolocalisation was assessed by fluorescence microscopy. Flow cytometry data were evaluated by analysis of variance. All three Panx proteins were found in dog spermatozoa: Panx1 was mostly localised to the acrosomal and equatorial segment, Panx2 was found in the posterior region of the head and tail and Panx3 was localised to the equatorial and posterior head segment. The percentage of PI-positive cells determined by flow cytometry was reduced ($P < 0.05$) in the presence of Panx inhibitors. These results show that Panx proteins are present in dog spermatozoa and increase PI permeability in frozen–thawed dog sperm, suggesting that the percentage of PI-positive spermatozoa used as an indicator of non-viable cells may lead to overestimation of non-viable cells.

Additional keywords: acrosome, cryopreservation, protein.

Received 5 July 2016, accepted 28 February 2017, published online 10 April 2017

Introduction

Semen cryopreservation is a useful tool for extending the viability of spermatozoa for long periods. This technique has an important role in conserving the genetic characteristics of domestic dogs and endangered canid species (Jewgenow and Songsasen 2014). However, cryopreserved sperm samples show decreased fertility compared with fresh spermatozoa because of damage to different sperm structures, such as the DNA, acrosome and plasma membrane, along with modifications of cellular functions, including a reduction in sperm motility (Palomino and De los Reyes 2009; Kim *et al.* 2010). These damages are related to stress conditions, such as intense osmotic, ionic and oxidative injures, and changes in plasma membrane permeability after freeze–thaw treatments (Mogas *et al.* 2011).

Several strategies have been studied to determine sperm quality and viability after freezing. Propidium iodide (PI) exclusion is the most common probe to determine cell viability by evaluating an increase in membrane permeability (Graham *et al.* 1990). Inside the cell, PI can intercalate with DNA and once the dye is bound to nucleic acids, its fluorescence is enhanced 20- to 50-fold. PI is widely used to determine cell viability as differences in plasma membrane integrity and permeability based on the capacity of living cells to exclude the dye (Yeh *et al.* 1981). It has been assumed that the ability of PI to penetrate a cell is dependent only upon the permeability of the plasma membrane, because PI does not stain live or early apoptotic cells due to the presence of an intact plasma membrane (Yeh *et al.* 1981; Lizama *et al.* 2009; Ortiz *et al.* 2009). In frozen–thawed dog sperm samples, PI exclusion shows a low percentage of viable spermatozoa (Corcini *et al.* 2016), but this marker does not correlate with fertilisation rates because samples with a high percentage of PI-positive cells still fertilised oocytes (Martins *et al.* 2009). It is therefore possible that PI can be incorporated through methods other than those associated with sperm damage.

In recent years, three pannexin proteins (Panx1, Panx2 and Panx3) have been described in different cells (Panchina *et al.* 2000; Bruzzone *et al.* 2003; Baranova *et al.* 2004; Vogt *et al.* 2005; Ray *et al.* 2006; Turmel *et al.* 2011). Pannexins form channels permeable to larger molecules, such as PI, ethidium bromide, 4′,6′-diamidino-2-phenylindole, ATP, small peptides and ions (Bao *et al.* 2004; Dourado *et al.* 2014). Pannexin channels are involved in ischaemia (Thompson *et al.* 2006;

Bargiotas *et al.* 2012; Xiong *et al.* 2014), inflammatory processes (Pelegrin and Surprenant 2006), neuronal communication (Li *et al.* 2012; Kranz *et al.* 2013), apoptosis (Chekeni *et al.* 2010; Xiao *et al.* 2012) and mechanical (Beckel *et al.* 2014) and osmotic stress (Voigt *et al.* 2015). In the reproductive tract of male rats, pannexins are expressed and regulated by androgens (Turmel *et al.* 2011); however, their expression in dog spermatozoa has not been reported. Although Panx1, Panx2 and Panx3 have been described in canine cells (Yen and Saier 2007), to our knowledge the presence of these proteins and their relationship with plasma membrane permeability in dog spermatozoa has not been described. Therefore, the aim of the present study was to evaluate the presence of pannexins in frozen–thawed dog spermatozoa using flow cytometry and indirect immunofluorescence, as well as their relationship with PI-positive spermatozoa after the freeze–thaw process.

Materials and methods

All animals used in the present study were treated according to guidelines of the Chilean Bioethics Committee of the Chilean Commission for Scientific and Technological Research (CONICYT) and the Ethics Committee of the Faculty of Veterinary Sciences, University of Chile.

Freeze–thawing of dog spermatozoa

Semen was collected twice using digital stimulation from eight adult (2–5 years old) pure or mixed-breed dogs. The sperm-rich fraction of each ejaculate was evaluated subjectively for progressive motility (using direct observation of a 10-μL aliquot of the sample at a magnification of ×200) and morphology using a phase contrast microscope; sperm concentration was measured by a haemocytometer as described previously (De los Reyes *et al.* 2009). Only samples with >80% progressive motility and ≤15% abnormal spermatozoa were selected for experiments. Three non-frozen sperm samples from different dogs were used as fresh controls.

Each sample was diluted 1 : 2 (v/v) in Tris buffer and centrifuged at 700*g* for 5 min at 21°C. The supernatant was discarded and the pellet resuspended in TRIS–citrate fructose freezing extender (De los Reyes *et al.* 2006). The sperm samples were loaded into 0.25-mL straws (IVM Technologies, France) for freezing at −196°C.

One straw from each dog was thawed in a water bath at 60°C for 8 s and the contents of each straw were placed in a different 1.5-mL tube. Fresh and thawed samples were washed by centrifugation at 700*g* for 5 min at 21°C, and 5×10^6 spermatozoa were resuspended in 700 μL non-capacitating SP-TALP medium (composition (in mM): KCl 3.1; $MgCl_2$ 0.4; NaCl 100; NaH_2PO_4 0.3; HEPES 10; sodium lactate 21.6; pyruvate 1; $CaCl_2$ 2, pH 7.2) without bovine serum albumin (BSA) or bicarbonate (Parrish *et al.* 1988).

Flow cytometry analysis of pannexin presence

Frozen–thawed dog spermatozoa (10^7 mL^{-1}) from each straw were fixed with 4% paraformaldehyde in phosphate-buffered saline (PBS; (in mM): NaCl 137; KCl 2.7; Na_2HPO_4 4.3; KH_2PO_4 1.47, pH 7.4) and washed with 1 mL PBS by centrifugation at 700*g* for 5 min at 21°C using an Eppendorf 5415D centrifuge. The samples were then permeabilised with PBS–0.1% Triton X-100 (Sigma Chemical) for 15 min at 21°C, washed twice with PBS–0.1% Tween (Sigma Chemical) and non-specific reaction sites blocked by PBS–3% BSA (Sigma Chemical)−1.5 μg mL^{-1} glycine (Winkler) for 1 h at room temperature. Then, samples were incubated with rabbit anti-Panx1 (1 : 200 dilution; AV42783; Sigma Chemical), rabbit anti-Panx2 (1 : 200 dilution; AV42778; Sigma Chemical) or rabbit anti-Panx3 (1 : 200 dilution; 433270; Thermo Fisher Scientific) antibodies at 4°C overnight. After overnight incubation, samples were washed three times with PBS–0.1% Tween for 5 min by centrifugation at 700*g* for 5 min and incubated with fluorescein isothiocyanate (FITC)-conjugated goat anti-rabbit antibody (Ab 7050; Abcam) for 3 h at 21°C. The samples were then washed three times with PBS–0.1% Tween and incubated for 15 min with 3 μM PI (Molecular Probes)−0.1% Tween–PBS at room temperature protected from the light, after which they were washed twice with PBS–0.1% Tween and resuspended in 1 mL PBS. Samples incubated without the primary antibody were used as negative controls, and spermatozoa that had not been incubated with secondary antibodies were used as autofluorescence controls.

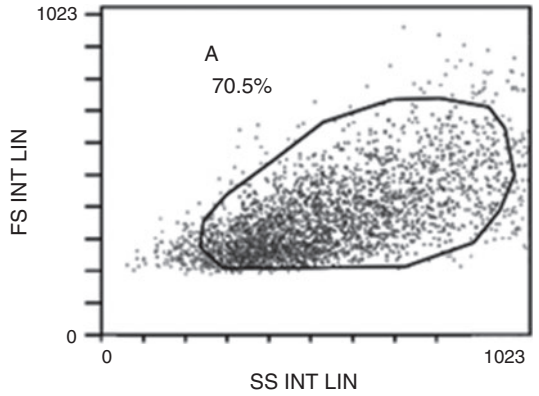

Fig. 1. Dot plot showing the discriminatory gate used forward scatter (FS; cell size) and side scatter (SS; cell complexity) to gate out debris. INT, integral signal; LIN, lineal gain.

Flow cytometry analysis was performed on a six-colour Gallius Cytometer (Beckman Coulter) with standard settings, including a compensation protocol for proper fluorophore discrimination. The cytometry settings included detection of forward scatter (FS) and side scatter (SS). FITC was detected at a wavelength of 500–550 nm in FL1, and PI was detected at a wavelength of 562–588 nm in FL3. During analysis, 20 000 events were classified into an FL1 and FL3 dot plot. Size gating was used to eliminate debris excluding low FS and SS events (Fig. 1). The percentage of PI-positive cells (events with PI fluorescence intensity ≥10°), FITC-positive cells (events with FITC fluorescence intensity ≥10°) and FITC and PI double-positive and -negative cells was calculated.

Indirect immunofluorescence

Aliquots of 2×10^6 frozen–thawed dog spermatozoa were fixed and washed with 1 mL PBS by centrifugation at 700*g* for 5 min

at 21°C, layered onto microscope slides and dried at 21°C. Spermatozoa were permeabilised with 0.3% Triton X-100–PBS for 15 min at 21°C. Non-specific reaction sites were blocked with 1 mL of 3% BSA–PBS for 1 h at 21°C and samples were incubated overnight with rabbit anti-Panx1, rabbit anti-Panx2 or rabbit anti-Panx3 antibodies (1 : 200 dilution for all) in a humidified chamber at 4°C. Samples were then washed three times with PBS–0.1% Tween and incubated with the secondary FITC-conjugated goat anti-rabbit antibody for 3 h at 21°C, washed three times in PBS–0.1% Tween for 5 min and incubated with 3 μM DAPI (4′,6′-diamidino-2-phenylindole)–0.1% Tween–PBS at room temperature for 10 min protected from the light. Thereafter, the samples were washed twice in PBS–0.1% Tween, mounted in Fluoromount aqueous mounting medium (Sigma) and observed under a Nikon Confocal Spectral C2 Eclipse Microscope. Spectral images in the 500–692 nm range captured with 488-nm laser excitation were used to detect pannexin localisation.

Flow cytometry PI assay

Sperm samples from each resuspended straw were divided into four (fresh) and seven (frozen–thawed) separate 2×10^6 mL^{-1} aliquots and each was incubated in 1 mL SP-TALP medium at 38°C for 10 min. Of the seven frozen–thawed aliquots, two were incubated with 15 μM carbenoxolone (CBX; Sigma Chemical), two were incubated with 1 mM probenecid (PBD; Thermo Fisher Scientific), two were incubated with 4 μL double-distilled water as a control and one aliquot was incubated with 4 μL SP-TALP as an autofluorescence control. All samples were incubated at 38°C for 15 min. Then, 3 μM PI alone or with 0.1% Triton X-100 (permeabilising agent) was added to one of the two samples in each treatment group and samples were incubated for a further 5 min under the same conditions. Triton X-100 (Sigma Chemical) permeabilised conditions were used as pannexin inhibitors/PI interaction controls. Unfixed and unwashed cell samples were used in these evaluations. The four fresh sperm sample aliquots were processed separately but subjected to the same four treatments, except for Triton X-100 exposure, as fresh sperm controls of pannexin.

Flow cytometry was performed as described above, with standard settings and FL3 detector activation. To determine levels of PI staining, 20 000 events in each tube were analysed. Histograms were obtained for each group and events were classified as PI-positive or PI-negative cells.

Statistical analysis

The percentage of PI-positive cells determined by flow cytometry was evaluated by analysis of variance (ANOVA). Groups with or without Triton X-100 permeabilisation, including the control group and the groups treated with the two inhibitors, were compared. When ANOVA showed statistically significant differences, results were subjected to Dunnett's post-hoc test to discriminate between treatment groups. These analyses were performed using GraphPad Prism 5.0 for Windows (GraphPad Software). Statistical significance was defined as $P < 0.05$.

Results

The presence and localisation of Panx1, Panx2 and Panx3 in dog spermatozoa was assessed by flow cytometry and indirect immunofluorescence analysis. According to the manufacturer (Sigma Chemical), the anti-Panx1 and anti-Panx2 antibodies used in the present study cross-react with dog pannexins. However, the anti-Panx3 antibody (Thermo Fisher Scientific) was designed using a synthetic peptide derived from mouse and rat Panx3 protein; therefore, the cross-reaction probability with canine Panx3 was estimated using BLASTp analysis comparing the canine Panx3 amino acid sequence (XP_852341.2) with mouse (NP_766042.2) and rat (NP_955430.1) sequences. These amino acid sequences were obtained using the respective Entrez Gene IDs (mouse: 208098; rat: 315567). The BLASTp analysis between canine and rat resulted in a query cover of 100%, generating an E-value $<1 \times 10 \times 10^{-6}$ with 90% identity. Between canine and mouse, the query cover was 99% with a similar E-value to that obtained with rat and 88% identity. These results lead us to believe that there is a high probability of cross-reaction of this antibody with canine Panx3.

Flow cytometry identification of pannexins

Gating settings for the sperm population (gated events) used to exclude non-sperm events are shown in Fig. 1.

Autofluorescence control (without secondary antibody or PI staining) showed that 95.9% of events were located in the lower left quadrant (no signal for PI or FITC; Fig. 2*a*). Negative control samples (without primary antibodies) did not show any signal (Fig. 2*b*). In all samples, PI staining was used as a fixed and permeabilised cell marker.

The cytometric analysis of frozen–thawed dog spermatozoa revealed the presence of pannexins. Positive signals were observed in the upper right quadrant, which showed that 78.3%, 85.9% and 81.6% of events were positively labelled for Panx1 (Fig. 2*c*), Panx2 (Fig. 2*d*) and Panx3 (Fig. 2*e*) respectively.

Presence of pannexins in sperm head and tail

Indirect immunofluorescence was used to determinate the subcellular localisation of Panx1, Panx2 and Panx3 in dog sperm samples. Positive staining for Panx1 was mostly found in the acrosomal region and equatorial segment (Fig. 3*a*, *c*), whereas the immunoreaction for Panx2 was primarily observed in the posterior region of the head and tail (Fig. 3*e*, *g*) and the immunosignal for Panx3 was located in the equatorial and posterior segment of the head (Fig. 3*i*, *k*). No signals were observed in any of the negative controls (Fig. 3*d*, *h*, *l*). In all samples, DAPI was used to counterstain DNA.

Effects of freeze–thawing on PI-positive cells

Dog spermatozoa were incubated with 3 μM PI to estimate the percentage of PI-positive spermatozoa using flow cytometry. A high percentage (79.7%) of PI-positive cells was found after freeze–thawing of control samples, when spermatozoa were incubated with vehicle (double-distilled water; see Fig. 4*a*). To evaluate the participation of pannexin channels in PI uptake in frozen–thawed spermatozoa, spermatozoa were incubated with one of two pannexin channel inhibitors, namely 15 μM CBX or 1 mM PBD, before the addition of PI. Then, flow cytometry was performed as described above. The results revealed that both

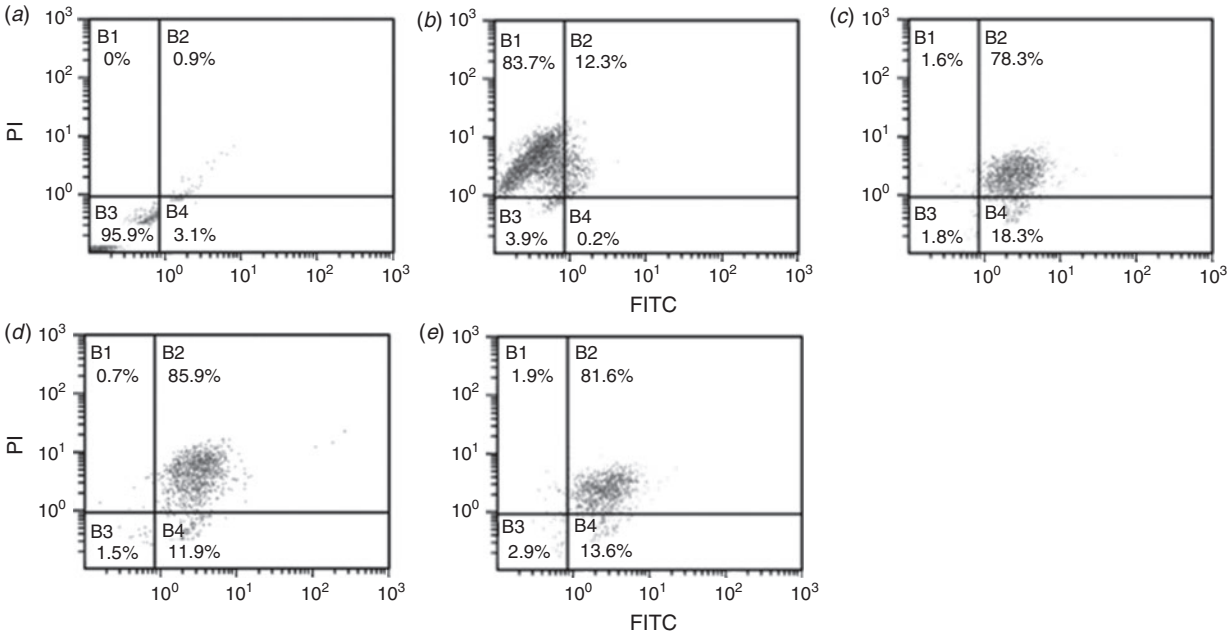

Fig. 2. Pannexins are present in dog spermatozoa. Representative plots showing (*a*) autofluorescence control (without secondary antibodies), (*b*) negative control (without primary antibodies), (*c*) pannexin (Panx) 1, (*d*) Panx2 and (*e*) Panx3. In all conditions, propidium iodide (PI) was used as the nuclear stain. FITC, fluorescein isothiocyanate.

CBX and PBD significantly prevented PI uptake, as shown in Fig. 4*b* and *c* respectively. The quantification of these results is shown in Fig. 4*d*. Fresh samples contained fewer PI-positive cells than frozen–thawed spermatozoa (Fig. 4*e*). No differences were observed when fresh samples were incubated with CBX (Fig. 4*f*) or PBD (Fig. 4*g*), with these results quantified in Fig. 4*h*.

To investigate whether the decrease in the percentage of PI-positive cells was due to an effective reduction of PI plasma membrane permeability and not by an interaction between the inhibitor and PI fluorescence, a permeabilising agent (0.1% Triton-X 100) was first added under similar experimental conditions. In these experiments, almost all permeabilised cells incubated with the vehicle incorporated PI (93.7%) with no significant effects of 15 μM CBX (92.1%) or 1 mM PBD (91.6%; Fig. 5).

Discussion

The present study reports, for the first time, the presence of Panx1, Panx2 and Panx3 in dog sperm samples. It is well established that there are several families of proteins capable of generating pores in the plasma membrane. In many cellular models, the pannexin family forms pores large enough to be permeable to large molecules such as PI (Ambrosi *et al.* 2010; Seminario-Vidal *et al.* 2011).

In determining sperm viability, PI exclusion has been the gold standard to assess damage to spermatozoa using microscopy or flow cytometry (Graham *et al.* 1990; Kim *et al.* 2013; Prochowska *et al.* 2014). It is hypothesised that PI only penetrates non-viable cells (Graham *et al.* 1990). Freezing and thawing result in a high percentage of damaged spermatozoa, causing a significant decrease in sperm viability and an increase in PI-positive cells.

Several studies in spermatozoa from dogs and other species have reported a high percentage of PI-positive cells in these assays, suggesting that these cells are dead spermatozoa (Dorado *et al.* 2013). In the present study we evaluated PI exclusion in frozen–thawed canine sperm samples and observed a high percentage of PI-positive cells, in accordance with previous reports (Dorado *et al.* 2013; Kim *et al.* 2013). This could be attributed to an increase in plasma membrane permeability caused by damage; however, this high rate was significantly reduced when spermatozoa were incubated with two pannexin channel inhibitors (CBX and PBD) before PI incubation, indicating that the pannexin channel mechanism may be involved in PI uptake. Therefore, not all PI-positive spermatozoa with high permeability to PI are dead cells. This result can be explained by the fact that the PI molecule is 14.5 ± 0.3 s.e.m Å wide (Orellana *et al.* 2011) and is able to pass through open pannexin channels that have a pore diameter of approximately 17–21 Å for Panx1 or 29.5–30.5 Å for Panx2 (Ambrosi *et al.* 2010).

The opening of pannexin channels could be related to plasma membrane mechanical stress (Bao *et al.* 2004; Beckel *et al.* 2014; Voigt *et al.* 2015) and changes in cytoskeletal organisation (Boyce *et al.* 2014) caused by cryopreservation (Gutiérrez-Pérez *et al.* 2011; Felipe-Pérez *et al.* 2012). Therefore, we cannot rule out sperm membrane damage, which could alter pannexin channels; however, the findings of the present study could suggest that the PI assay underestimates the percentage

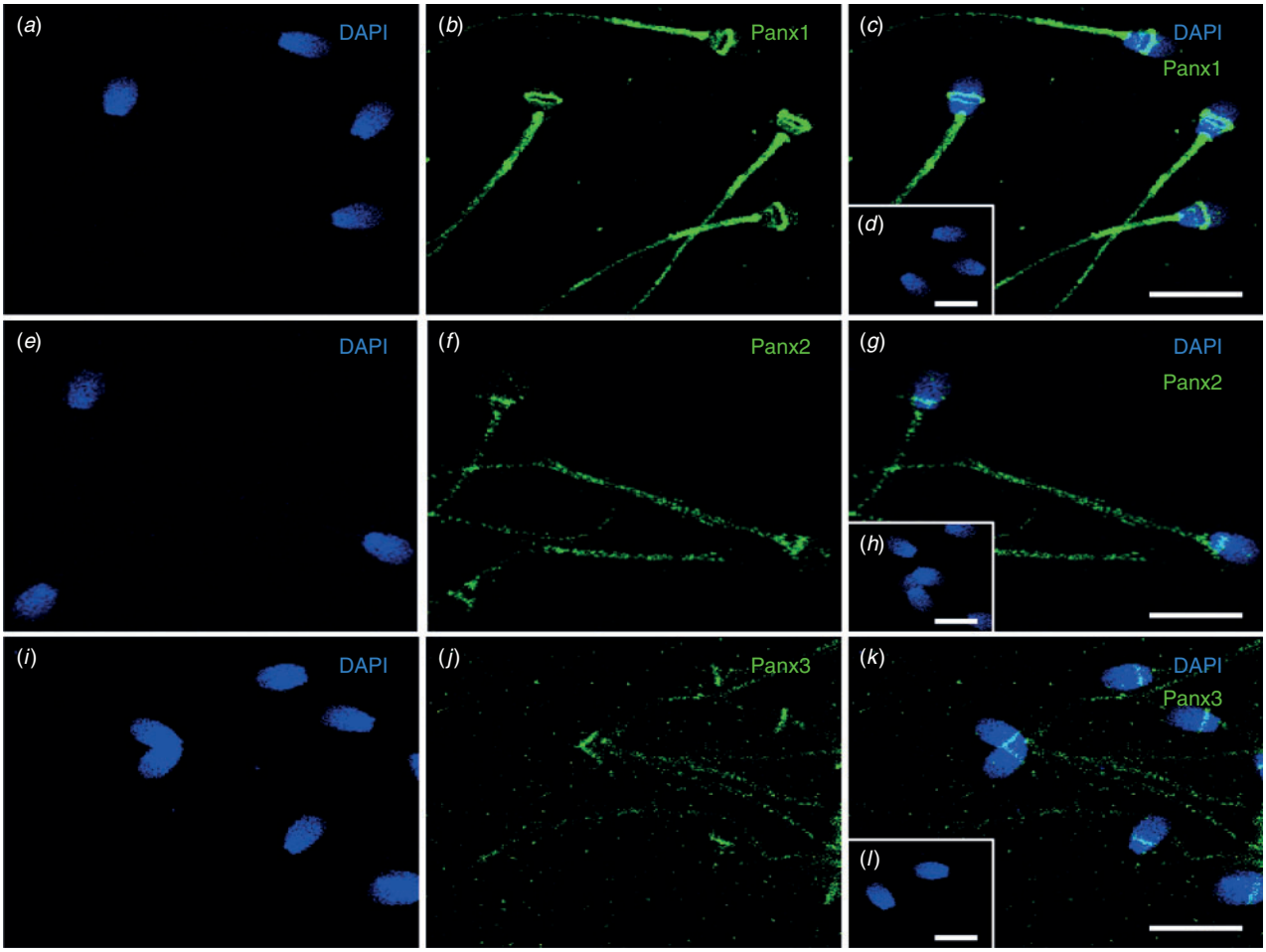

Fig. 3. Subcellular localisation of pannexins in dog spermatozoa. Representative immunofluorescence images of (*a–c*) pannexin (Panx) 1, (*e–g*) Panx2 and (*i–k*) Panx3 staining. Nuclei were counterstained (blue) with 4′,6′-diamidino-2-phenylindole (DAPI). Strong Panx1 staining (green) is observed in the equatorial region of the head, nucleus and brightfield image, whereas Panx2 staining is mostly localised to the posterior region of the head and tail, and the immunosignal for Panx3 is seen in the equatorial and posterior region of the head. (*d*, *h*, *l*) Brightfield images of dog spermatozoa incubated without the primary antibody (negative control), with nuclei stained blue. Scale bars = 20 μm.

of live cells; that is, the PI assay has a 20% chance of detecting false-positives on flow cytometry.

The presence of pannexins in dog spermatozoa raises the question of the physiological function of these protein channels in dog spermatozoa. Many studies have indicated that pannexins are important channels in the physiology and pathophysiology of different tissues. These proteins are involved in the release of large molecules, such as ATP (Bao *et al.* 2004; Krick *et al.* 2016) and arachidonic acid (Jiang *et al.* 2007), as well as in purinergic signalling (Bond and Naus 2014). Pannexins could act as non-selective channels for calcium, sodium, potassium or bicarbonate, ions related to mammalian sperm capacitation and the acrosome reaction (Bond and Naus 2014). Because the localisation of pannexins showed compartmentalised distribution in dog spermatozoa, it could be that these proteins participate in different steps of the capacitation processes. Panx1 and Panx3 were located in the equatorial head segment, which has been linked to the acrosome reaction and oocyte interaction (Cuasnicú *et al.* 2016; Stival *et al.* 2016). Meanwhile, Panx2 was limited to the midpiece of the tail, suggesting that signalling events are required for hyperactivated motility (Stival *et al.* 2016). Hyperactivation is a phenomenon that causes changes in sperm motility and is characterised by large asymmetrical bends at the proximal midpiece of the tail (Stival *et al.* 2016). This movement is initiated by increases in calcium levels that lead to increased cAMP in the cytoplasm of the sperm tail (Ishijima 2015). Because both the acrosome reaction and hyperactivated motility are ion exchange-dependent processes (Santi *et al.* 2013), pannexins could be involved in mammalian sperm capacitation.

In addition, canine spermatozoa show a high percentage of spontaneous acrosome reactions (Kawakami *et al.* 1993), which is increased in cryopreserved samples (Peña *et al.* 2004). This condition could be explained by the ability of pannexin channels to allow the ion influx necessary for acrosomal exocytosis (Sánchez-Cárdenas *et al.* 2014). Therefore, calcium

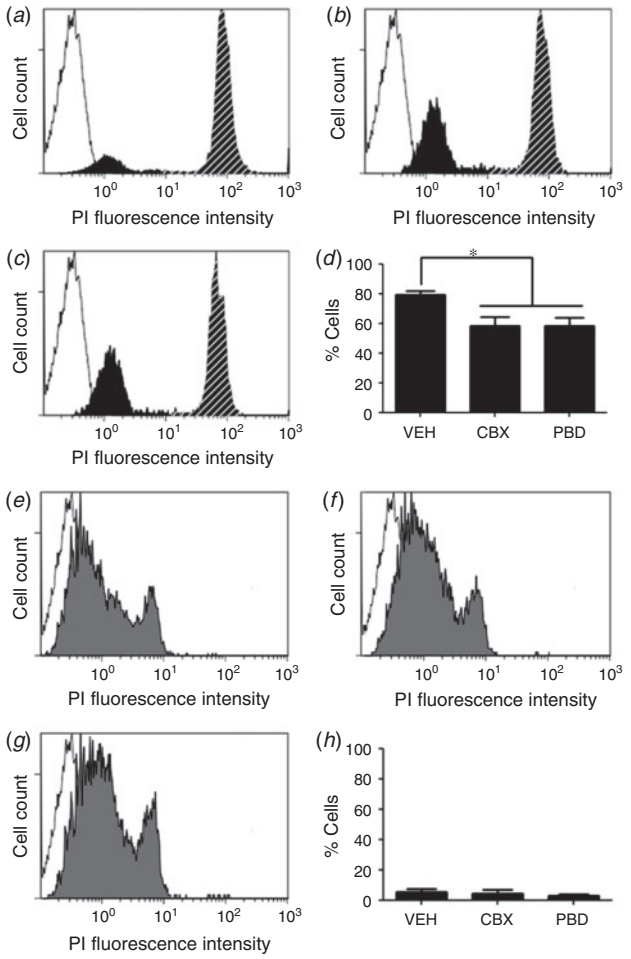

Fig. 4. Effects of freeze–thawing on the number of propidium iodide (PI)-positive cells and role of pannexin channels. (*a–c*) Representative histograms show results for frozen–thawed dog spermatozoa preincubated with (*a*) vehicle (control; VEH) and PI, (*b*) the pannexin channel inhibitor carbenoxolone (CBX) and PI and (*c*) the pannexin channel inhibitor probenecid (PBD) and PI. (*d*) Summary of results, showing the mean ± s.d. percentage of PI-positive frozen–thawed cells in the three groups ($n = 8$). (*e–g*) Representative histograms showing results for fresh dog sperm samples preincubated with (*e*) vehicle (control) and PI, (*f*) CBX and PI and (*g*) PBD and PI. (*h*) Summary of results, showing the mean ± s.d. percentage of PI-positive fresh spermatozoa in the three groups ($n = 3$). *$P < 0.05$ (ANOVA with Dunnett's post hoc test).White curve, autofluorescence control; black curve, PI-negative frozen–thawed spermatozoa; hatched curve, PI-positive frozen–thawed spermatozoa; grey curve, PI-negative fresh spermatozoa.

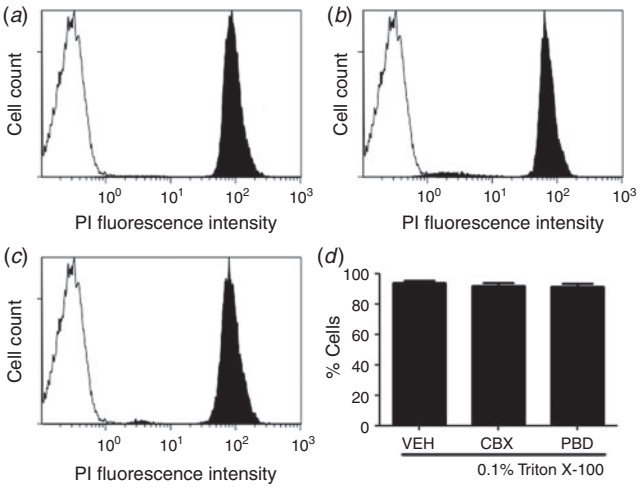

Fig. 5. Effects of the pannexin channel inhibitors on the percentage of permeabilised propidium iodide (PI)-positive cells. Representative histograms show results for permeabilised dog spermatozoa preincubated with (*a*) vehicle control (VEH) and PI, (*b*) carbenoxolone (CBX) and PI and (*c*) probenecid (PBD) and PI. White curve, autofluorescence control; black curve, experimental condition. (*d*) Mean ± s.e.m. percentage of PI-positive cells in the different groups ($n = 8$). No significant differences were found between the different treatments (ANOVA).

levels may be deregulated in spermatozoa with open pannexin channels, inducing a premature acrosome reaction. Further studies are required to determine the roles of pannexins in dog spermatozoa, and this knowledge will be important when using reproductive freezing technologies in canines.

In conclusion, pannexins are present in dog spermatozoa, suggesting the participation of pannexin channels in the increase in PI permeability after cryopreservation in dog spermatozoa. These findings indicate that the percentage of PI-positive spermatozoa classified as non-viable cells may be an overestimate of the number of non-viable cells. Further studies should clarify this point.

Acknowledgements

This research was supported by Grants 1140658 (FONDECYT) and EQM120156 (FONDEQUIP) from the National Commission for Scientific and Technological Research, Chile (CONICYT).

References

Ambrosi, C., Gassmann, O., Pranskevich, J. N., Boassa, D., Smock, A., Wang, J., Dahl, G., Steinem, C., and Sosinsky, G. E. (2010). Pannexin1 and Pannexin2 channels show quaternary similarities to connexons and different oligomerization numbers from each other. *J. Biol. Chem.* **285**, 24420–24431. doi:10.1074/JBC.M110.115444

Bao, L., Locovei, S., and Dahl, G. (2004). Pannexin membrane channels are mechanosensitive conduits for ATP. *FEBS Lett.* **572**, 65–68. doi:10.1016/J.FEBSLET.2004.07.009

Baranova, A., Ivanov, D., Petrash, N., Pestova, A., Skoblov, M., Kelmanson, I., Shagin, D., Nazarenko, S., Geraymovych, E., Litvin, O., Tiunova, A., Born, T., Usman, N., Staroverov, D., Lukyanov, S., and Panchin, Y. (2004). The mammalian pannexin family is homologous to the invertebrate innexin gap junction proteins. *Genomics* **83**, 706–716. doi:10.1016/J.YGENO.2003.09.025

Bargiotas, P., Krenz, A., Monyer, H., and Schwaninger, M. (2012). Functional outcome of pannexin-deficient mice after cerebral ischemia. *Channels (Austin)* **6**, 453–456. doi:10.4161/CHAN.22315

Beckel, J. M., Argall, A. J., Lim, J. C., Xia, J., Lu, W., Coffey, E. E., Macarak, E. J., Shahidullah, M., Delamere, N. A., Zode, G. S., Sherffield, V. C., Shestopalov, V. I., Laties, A. M., and Mitchell, C. H. (2014). Mechanosensitive release of adenosine 5′-triphosphate through pannexin channels and mechanosensitive upregulation of pannexin channels in optic nerve head astrocytes: a mechanism for purinergic

involvement in chronic strain. *Glia* **62**, 1486–1501. doi:10.1002/GLIA.22695

Bond, S. R., and Naus, C. C. (2014). The pannexins: past and present. *Front. Physiol.* **5**, 58. doi:10.3389/FPHYS.2014.00058

Boyce, A. K., Wicki-Stordeur, L. E., and Swayne, L. A. (2014). Powerful partnership: crosstalk between pannexin 1 and the cytoskeleton. *Front. Physiol.* **5**, 27. doi:10.3389/FPHYS.2014.00027

Bruzzone, R., Hormuzdi, S., Barbe, M., and Monyer, H. (2003). Pannexins, a family of gap junction proteins expressed in brain. *Proc. Natl Acad. Sci. USA* **100**, 13644–13649. doi:10.1073/PNAS.2233464100

Chekeni, F. B., Elliott, M. R., Sandilos, J. K., Walk, S. F., Kinchen, J. M., Lazarowski, E. R., Armstrong, A. J., Penuela, S., Laird, D. W., Salvesen, G. S., Isakson, B. E., Bayliss, D. A., and Ravichandran, K. S. (2010). Pannexin 1 channels mediate 'find-me' signal release and membrane permeability during apoptosis. *Nature* **467**, 863–867. doi:10.1038/NATURE09413

Corcini, C. D., Goularte, K. L., Bongalhardo, D. C., Lucia, T., Jr, Jardim, R. D., and Varela, A. S., Junior (2016). Effect of egg yolk plasma on dog sperm cryopreservation. *Andrologia* **48**, 114–115. doi:10.1111/AND.12411

Cuasnicú, P. S., Da Ros, V. G., Weigel-Muñoz, M., and Cohen, D. J. (2016). Acrosome reaction as a preparation for gamete fusion. *Adv. Anat. Embryol. Cell Biol.* **220**, 159–172. doi:10.1007/978-3-319-30567-7_9

De los Reyes, M., Carrion, R., and Barros, C. (2006). *In vitro* fertilization of *in vitro* matured canine oocytes using frozen–thawed dog semen. *Theriogenology* **66**, 1682–1684. doi:10.1016/J.THERIOGENOLOGY.2006.02.002

De los Reyes, M., de Lange, J., Anguita, C., Palomino, J., and Barros, C. (2009). *In vitro* sperm penetration through the zona pellucida of immature and *in vitro* mature canine oocytes using fresh, chilled and frozen dog semen. *Anim. Reprod. Sci.* **110**, 37–45. doi:10.1016/J.ANIREPROSCI.2007.12.010

Dorado, J., Gálvez, M. J., Morrell, J. M., Alcaráz, L., and Hidalgo, M. (2013). Use of single-layer centrifugation with Androcoll-C to enhance sperm quality in frozen–thawed dog semen. *Theriogenology* **80**, 955–962. doi:10.1016/J.THERIOGENOLOGY.2013.07.027

Dourado, M., Wong, E., and Hackos, D. H. (2014). Pannexin-1 is blocked by its C-terminus through a delocalized non-specific interaction surface. *PLoS One* **9**, e99596. doi:10.1371/JOURNAL.PONE.0099596

Felipe-Pérez, Y. E., Valencia, J., Juárez-Mosqueda, Mde. L., Pescador, N., Roa-Espitia, A. L., and Hernández-González, E. O. (2012). Cytoskeletal proteins F-actin and β-dystrobrevin are altered by the cryopreservation process in bull sperm. *Cryobiology* **64**, 103–109. doi:10.1016/J.CRYOBIOL.2011.12.004

Graham, J. K., Kunze, E., and Hammerstedt, R. H. (1990). Analysis of sperm cell viability, acrosomal integrity, and mitochondrial function using flow cytometry. *Biol. Reprod.* **43**, 55–64. doi:10.1095/BIOLREPROD43.1.55

Gutiérrez-Pérez, O., Juárez-Mosqueda, M. L., Mota, D., and Trujillo, M. E. (2011). The disruption in actin–perinuclear theca interactions are related with changes induced by cryopreservation observed on sperm chromatin nuclear decondensation of boar semen. *Cryobiology* **62**, 32–39. doi:10.1016/J.CRYOBIOL.2010.11.006

Ishijima, S. (2015). Ca^{2+} and cAMP regulations of microtubule sliding in hyperactivated motility of bull spermatozoa. *Proc. Jpn. Acad. Ser. B Phys. Biol. Sci.* **91**, 99–108. doi:10.2183/PJAB.91.99

Jewgenow, K., and Songsasen, N. (2014). Reproduction and advances in reproductive studies in carnivores. *Adv. Exp. Med. Biol.* **753**, 205–239. doi:10.1007/978-1-4939-0820-2_10

Jiang, H., Zhu, A. G., Mamczur, M., Falck, J. R., Lerea, K. M., and McGiff, J. C. (2007). Stimulation of rat erythrocyte P2X7 receptor induces the release of epoxyeicosatrienoic acids. *Br. J. Pharmacol.* **151**, 1033–1040. doi:10.1038/SJ.BJP.0707311

Kawakami, E., Vandevoort, C. A., Mahi-Brown, C. A., and Overstreet, J. W. (1993). Induction of acrosome reactions of canine sperm by homologous zona pellucida. *Biol. Reprod.* **48**, 841–845. doi:10.1095/BIOLREPROD48.4.841

Kim, S. H., Yu, D. H., and Kim, Y. J. (2010). Effects of cryopreservation on phosphatidylserine translocation, intracellular hydrogen peroxide, and DNA integrity in canine sperm. *Theriogenology* **73**, 282–292. doi:10.1016/J.THERIOGENOLOGY.2009.09.011

Kim, H. H., Funaro, M., Mazel, S., Goldstein, M., Schlegel, P. N., and Paduch, D. A. (2013). Flow cytometric characterization of apoptosis and chromatin damage in spermatozoa. *Reprod. Biomed. Online* **26**, 393–395. doi:10.1016/J.RBMO.2012.12.005

Kranz, K., Dorgau, B., Pottek, M., Herrling, R., Schultz, K., Bolte, P., Monyer, H., Penuela, S., Laird, D. W., Dedek, K., Weiler, R., and Janssen-Bienhold, U. (2013). Expression of Pannexin1 in the outer plexiform layer of the mouse retina and physiological impact of its knockout. *J. Comp. Neurol.* **521**, 1119–1135. doi:10.1002/CNE.23223

Krick, S., Wang, J., St-Pierre, M., Gonzalez, C., Dahl, G., and Salathe, M. (2016). Dual oxidase 2 (Duox2) regulates pannexin 1-mediated ATP release in primary human airway epithelial cells via changes in intracellular pH and not H_2O_2 production. *J. Biol. Chem.* **291**, 6423–6432. doi:10.1074/JBC.M115.664854

Li, Y., Du, X. F., Liu, C. S., Wen, Z. L., and Du, J. L. (2012). Reciprocal regulation between resting microglial dynamics and neuronal activity *in vivo*. *Dev. Cell* **23**, 1189–1202. doi:10.1016/J.DEVCEL.2012.10.027

Lizama, C., Lagos, C. F., Lagos-Cabré, R., Cantuarias, L., Rivera, F., Huenchuñir, P., Pérez-Acle, T., Carrión, F., and Moreno, R. D. (2009). Calpain inhibitors prevent p38 MAPK activation and germ cell apoptosis after heat stress in pubertal rat testes. *J. Cell. Physiol.* **221**, 296–305. doi:10.1002/JCP.21868

Martins, M. I. M., Padilha, L. C., Souza, F. F., and Lopes, M. D. (2009). Fertilizing capacity of frozen epididymal sperm collected from dogs. *Reprod. Domest. Anim.* **44**, 342–344. doi:10.1111/J.1439-0531.2009.01431.X

Mogas, M. T., Alamo, M. R., and Rodríguez-Gil, J. E. (2011). Roles of Na^+/K^+-dependent ATPase, Na^+/H^+ antiporter and GLUT hexose transporters in the cryosurvival of dog spermatozoa: effects on viability, acrosome state and motile sperm subpopulation structure. *Theriogenology* **75**, 1669–1681. doi:10.1016/J.THERIOGENOLOGY.2010.12.030

Orellana, J. A., Díaz, E., Schalper, K. A., Vargas, A. A., Bennett, M. V., and Sáez, J. C. (2011). Cation permeation through connexin 43 hemichannels is cooperative, competitive and saturable with parameters depending on the permeant species. *Biochem. Biophys. Res. Commun.* **409**, 603–609. doi:10.1016/J.BBRC.2011.05.031

Ortiz, R. J., Lizama, C., Codelia, V. A., and Moreno, R. D. (2009). A molecular evaluation of germ cell death induced by etoposide in pubertal rat testes. *Mol. Hum. Reprod.* **15**, 363–371. doi:10.1093/MOLEHR/GAP024

Palomino, J., and De los Reyes, M. (2009). A scanning electron microscope study of frozen/thawed dog sperm during *in vitro* gamete interaction. *Reprod. Domest. Anim.* **44**, 278–283. doi:10.1111/J.1439-0531.2008.01063.X

Panchina, Y., Kelmanson, I., Matz, M., Lukyanov, K., Usman, N., and Lukyanov, S. (2000). A ubiquitous family of putative gap junction molecules. *Curr. Biol.* **10**, R473–R474. doi:10.1016/S0960-9822(00)00576-5

Parrish, J. J., Susko-Parrish, J., Winer, M. A., and First, N. L. (1988). Capacitation of bovine sperm by heparin. *Biol. Reprod.* **38**, 1171–1180. doi:10.1095/BIOLREPROD38.5.1171

Pelegrin, P., and Surprenant, A. (2006). Pannexin-1 mediates large pore formation and interleukin-1beta release by the ATP-gated P2X7 receptor. *EMBO J.* **25**, 5071–5082. doi:10.1038/SJ.EMBOJ.7601378

Peña, A. I., Barrio, M., Becerra, J. J., Quintela, P. G., and Herradón, P. G. (2004). Zona pellucida binding ability and responsiveness to ionophore challenge of cryopreserved dog spermatozoa after different periods of capacitation *in vitro*. *Anim. Reprod. Sci.* **84**, 193–210. doi:10.1016/J.ANIREPROSCI.2003.11.007

Prochowska, S., Niżański, W., Ochota, M., and Partyka, A. (2014). Effect of dilution rate on feline urethral sperm motility, viability, and DNA integrity. *Theriogenology* **82**, 1273–1280. doi:10.1016/J.THERIOGENOLOGY.2014.08.012

Ray, A., Zoidl, G., Wahle, P., and Dermietzel, R. (2006). Pannexin expression in the cerebellum. *Cerebellum* **5**, 189–192. doi:10.1080/14734220500530082

Sánchez-Cárdenas, C., Servín-Vences, M. R., José, O., Treviño, C. L., Hernández-Cruz, A., and Darszon, A. (2014). Acrosome reaction and Ca^{2+} imaging in single human spermatozoa: new regulatory roles of $[Ca^{2+}]_i$. *Biol. Reprod.* **91**, 67. doi:10.1095/BIOLREPROD.114.119768

Santi, C. M., Orta, G., Salkoff, L., Visconti, P. E., Darszon, A., and Treviño, C. L. (2013). K^+ and Cl^- channels and transporters in sperm function. *Curr. Top. Dev. Biol.* **102**, 385–421. doi:10.1016/B978-0-12-416024-8.00014-3

Seminario-Vidal, L., Okada, S. F., Sesma, J. I., Kreda, S. M., van Heusden, C. A., Zhu, Y., Jones, L. C., O'Neal, W. K., Penuela, S., Laird, D. W., Boucher, R. C., and Lazarowski, E. R. (2011). Rho signaling regulates pannexin 1-mediated ATP release from airway epithelia. *J. Biol. Chem.* **286**, 26277–26286. doi:10.1074/JBC.M111.260562

Stival, C., Puga Molina, Ldel. C., Paudel, B., Buffone, M. G., Visconti, P. E., and Krapf, D. (2016). Sperm capacitation and acrosome reaction in mammalian sperm. *Adv. Anat. Embryol. Cell Biol.* **220**, 93–106. doi:10.1007/978-3-319-30567-7_5

Thompson, R. J., Zhou, N., and MacVicar, B. A. (2006). Ischemia opens neuronal gap junction hemichannels. *Science* **312**, 924–927. doi:10.1126/SCIENCE.1126241

Turmel, P., Dufresne, J., Hermo, L., Smith, C., Penuela, S., Laird, D., and Cyr, D. (2011). Characterization of pannexin1 and pannexin3 and their regulation by androgens in the male reproductive tract of the adult rat. *Mol. Reprod. Dev.* **78**, 124–138. doi:10.1002/MRD.21280

Vogt, A., Hormuzdi, S., and Monyer, H. (2005). Pannexin1 and Pannexin2 expression in the developing and mature rat brain. *Brain Res. Mol. Brain Res.* **141**, 113–120. doi:10.1016/J.MOLBRAINRES.2005.08.002

Voigt, J., Grosche, A., Vogler, S., Pannicke, Y., Hollborn, M., Kohen, L., Wiedemann, P., Reinchenbach, A., and Bringmann, A. (2015). Non-vesicular release of ATP from rat retinal glial (Müller) cells is differentially mediated in response to osmotic stress and glutamate. *Neurochem. Res.* **40**, 651–660. doi:10.1007/S11064-014-1511-Z

Xiao, F., Waldrop, S. L., Khimji, A. K., and Kilic, G. (2012). Pannexin1 contributes to pathophysiological ATP release in lipoapoptosis induced by saturated free fatty acids in liver cells. *Am. J. Physiol. Cell Physiol.* **303**, C1034–C1044. doi:10.1152/AJPCELL.00175.2012

Xiong, X. X., Gu, L. J., Shen, J., Kang, X. H., Zheng, Y. Y., Yue, S. B., and Zhu, S. M. (2014). Probenecid protects against transient focal cerebral ischemic injury by inhibiting HMGB1 release and attenuating AQP4 expression in mice. *Neurochem. Res.* **39**, 216–224. doi:10.1007/S11064-013-1212-Z

Yeh, C. J., Hsi, B. L., and Faulk, W. P. (1981). Propidium iodide as a nuclear marker in immunofluorescence. II. Use with cellular identification and viability studies. *J. Immunol. Methods* **43**, 269–275. doi:10.1016/0022-1759(81)90174-5

Yen, M. R., and Saier, M. H., Jr (2007). Gap junctional proteins of animals: the innexin/pannexin superfamily. *Prog. Biophys. Mol. Biol.* **94**, 5–14. doi:10.1016/J.PBIOMOLBIO.2007.03.006